Double-Rydberg Anions: Predictions on $NH_3AH_n^-$ and $OH_2AH_n^-$ Structures

Hugh Hopper, Michael Lococo, O. Dolgounitcheva, V. G. Zakrzewski, and J. V. Ortiz*

Contribution from the Department of Chemistry, Kansas State University, Manhattan, Kansas 66506-3701

Received June 26, 2000. Revised Manuscript Received October 26, 2000

Abstract: Double−Rydberg anions consist of a closed-shell cationic core and two electrons in diffuse orbitals. In addition to the already characterized tetrahedral NH_4^- and pyramidal OH_3^-, the list of stable double-Rydberg anions includes members of the NH_3R^- and OH_2R^- sets (where R = F, OH, NH_2, and CH_3) considered here. Double-Rydberg isomers of NH_3OH^-, $NH_3\,NH_2^-$, $NH_3CH_3^-$, and $OH_2CH_3^-$ are stable minima in their potential energy surfaces and have positive, vertical electron detachment energies. Similar structures have been found for the corresponding neutrals, which all have adiabatic electron affinities that are greater than zero. Dyson orbitals pertaining to the least bound electrons of the NH_3R^- and OH_2R^- anions are distributed chiefly outside the N−H and O−H bonds of the tetrahedral nitrogen and pyramidal oxygen atoms.

Introduction

Thorough computational exploration of anionic potential energy surfaces and innovation of techniques for generating and characterizing gas-phase anions may both lead to the discovery of novel patterns of chemical bonding. In the case of double-Rydberg anions, experimental examination of anion−molecule complexes produced unusual features in photoelectron spectra that corresponded to unstable, but theoretically characterized structures.

The first photoelectron experiment performed on an anion−molecule complex was Bowen's study on NH_4^-.[1] With proper adjustment of source conditions, this anion may be generated by electron injection from a hot filament into an expanding supersonic jet. In this experiment, a mass-selected ion beam, crossed with a fixed-frequency laser, produces photoelectrons that are analyzed with respect to energy. Bowen ascribed his principal peak (A) to electron detachment from H^- coordinated to NH_3. A similar description of NH_4^- had accompanied a Fourier-transform, ion-cyclotron spectrum.[2] An additional peak (B) with much lower intensity was displaced from the A peak by an amount close to a vibrational excitation energy on NH_3.

But for the thoroughness of these workers, the matter might have ended there. Careful inspection of the low electron binding energy region of the spectrum revealed a feature (C) that was clearly visible only after expansion of the ordinate (photoelectron counts) by a factor of 30.[3] This sharp peak, unlike the B peak, did not change position in the ND_4^- spectrum and its intensity, relative to the A peak, was sensitive to conditions in the ion source. Bowen proposed that the C peak belonged to a tetrahedral species.[4−6] Some theoretical support for the tetrahedral anion proposal existed as well, for two publications had reported such structures in the potential energy surface of NH_4^-.[7,8]

Subsequent calculations showed that these spectral features indeed correspond to $H^-(NH_3)$ and tetrahedral structures. Electron propagator calculations on the vertical detachment energies of the anions were within 0.05 eV of the A and C peaks after a thorough exhaustion of basis set and correlation effects.[9] (Vibrational frequencies also explained the position of the B peak.) Information on geometries, dissociation energies, relaxation energies, and other parameters also lent credibility to the calculated results. The sharpness of the C peak was explained by an analysis of the Dyson orbital connecting the tetrahedral NH_4^- anion and the corresponding neutral. This a_1 orbital's radial structure and its N−H antibonding and H−H bonding relationships accounted for the small difference between the vertical and adiabatic electron detachment energies. The shape of the Dyson orbital also validated Simons and Gutowski's use of the term double-Rydberg anion (see ref 10 for a review), for two electrons are found in a Rydberg-like orbital that is distributed on the periphery of a closed-shell cation, NH_4^+. A parallel study employing configuration interaction soon followed from the Utah group and close agreement on the electron detachment energy of tetrahedral NH_4^- resulted.[11,12] Matsunaga and Gordon have confirmed these conclusions and have performed classical trajectory calculations on dissociation pathways.[13]

Are there other double-Rydberg anions? Theory says yes. Qualitative interpretation of the Dyson orbital for electron detachment from tetrahedral NH_4^- stimulated investigation of other closed-shell cations with two, diffuse electrons assigned to orbitals that transform according to the totally symmetric,

(1) Coe, J. V.; Snodgrass, J. T.; Freidhoff, C. B.; McHugh, K. M.; Bowen, K. H. *J. Chem. Phys.* **1985**, *83*, 3169.
(2) Kleingeld, J. C.; Ingemann, S.; Jalonen, J. E.; Nibbering, N. M. M. *J. Am. Chem. Soc.* **1983**, *105*, 2474.
(3) Snodgrass, J. T.; Coe, J. V.; Freidhoff, C. B.; McHugh K. M.; Bowen, K. H. *Faraday Discuss. Chem. Soc.* **1988**, *86*, 241.
(4) Snodgrass, J. T. Ph.D. dissertation, Johns Hopkins University, 1986.
(5) Coe, J. V. Ph.D. dissertation, Johns Hopkins University, 1986.
(6) Arnold, S. T.; Eaton, J. G.; Patel-Misra, D.; Sarkas, H. W.; Bowen, K. H. In *Ion and Cluster Ion Spectroscopy and Structure*; Maier, J. P., Ed.; Elsevier: Amsterdam, 1988; p 147.
(7) Cardy, H.; Larrieu C.; Dargelos, A. *Chem. Phys. Lett.* **1986**, *131*, 507.
(8) Cremer, D.; Kraka, E. *J. Phys. Chem.* **1986**, *90*, 33.
(9) Ortiz, J. V. *J. Chem. Phys.* **1987**, *87*, 3557.
(10) Simons, J.; Gutowski, M. *Chem. Rev.* **1991**, *91*, 669.
(11) Gutowski, M.; Simons, J.; Hernández R.; Taylor, H. L. *J. Phys. Chem.* **1988**, *92*, 6179.
(12) Gutowski, M.; Simons, J. *J. Chem. Phys.* **1990**, *93*, 3874.
(13) Matsunaga, N.; Gordon, M. S. *J. Phys. Chem.* **1995**, *99*, 12773.

10.1021/ja002292+ CCC: $19.00
Published on Web 12/05/2000

irreducible representation of the cation's point group. Among the predicted double-Rydberg anions are a pyramidal (C_{3v}) form of OH_3^- [12,14] and tetrahedral PH_4^-.[15] The latter anion also has a C_{2v} form of lower energy in which the five sites of a trigonal bipyramid centered on P are occupied by four P−H bonds and an equatorial lone pair. Gordon[13] and Morokuma[16] have confirmed these results. (An earlier study of PH_4^- that was interpreted in terms of valence-shell, electron-pair repulsion theory was made by Trinquier et al.[17]) Extensive searches on the potential energy surfaces of FH_2^-, ClH_2^-, and SH_3^- found no double-Rydberg minima.[15] Simons, Gutowsky, and coworkers reached similar conclusions on OH_3^- and FH_2^-.[10] They also have examined NeH^-, CH^-, and H_3^- without finding a stable double-Rydberg isomer. Wang and Boyd have analyzed the electronic densities and properties of NH_4^- and OH_3^-.[18] Two papers have examined the possibility of chemical binding between two NH_4 Rydberg molecules[19,20] and another considered ionic bonding between alkali cations and double-Rydberg anions.[21] $NH_{4-n}(CH_3)_n$ Rydberg radicals with $n = 1-4$ have been studied as well.[22]

In this work, the existence of NH_3R^- and OH_2R^- double-Rydberg anions, where R = H, F, OH, NH_2, and CH_3, is considered. Satisfaction of two criteria is sought. First, the anion must be a minimum in its potential energy surface. Second, the vertical, electron-detachment energy (VEDE) calculated for the anion must be greater than zero. Finally, the adiabatic electron binding energy (AEDE) of each candidate anion is examined.

Methods

Geometry optimizations and frequency calculations were done initially at the Hartree−Fock (HF) level of theory, using the 6-31G(d,p) basis set[23−25] for cations and the 6-31++G(d,p) basis set[23−26] for neutrals and anions. Diffuse and polarization functions were especially important for neutrals and anions because of the diffuse nature of the highest occupied molecular orbital. Optimizations and harmonic frequency calculations then were done at the second-order, many-body perturbation theory, or Møller−Plesset second-order (MP2), level[27] using the 6-311++G(d,p) basis set[26,28] for all molecules and ions. The same basis set was used for optimizations and frequency calculations with the so-called quadratic configuration interaction with the single and doubles (QCISD) total energy procedure.[29] A single-point calculation was performed on each neutral molecule at the optimized geometry of the corresponding anion, thus permitting calculation of a neutral relaxation energy (RE). Anion VEDEs were calculated with the P3 electron propagator method[30] at the anion minima. Here, the 6-311++G(2df,2p) basis was supplemented with an additional set of s and p functions on non-hydrogen atoms and an additional set of s functions on hydrogen atoms. The ++ exponents were multiplied by $^1/_3$ to generate the exponents of the additional functions. To confirm the perturbative, P3 results, electron propagator calculations with a Brueckner doubles, coupled-cluster reference state[31,32] were performed for some anions with the aug-cc-pVTZ[33] basis sets. These calculations were repeated for NH_4^- and OH_3^- with added s, p, d, and f functions on non-hydrogen nuclei and with s, p, and d functions on hydrogens whose exponents differ from the most diffuse exponents of the aug-cc-pVTZ basis by the same $^1/_3$ factor. Only 1s core molecular orbitals are dropped from propagator summations.

All electronic structure calculations were executed with Gaussian 98[34] and with newly developed electron propagator links.

In electron propagator calculations, Dyson orbitals corresponding to electron binding energies are generated. For an initial state, Ψ_N, with N electrons and a final state, Ψ_{N-1}, with one fewer electron, the Dyson orbital, $\psi^{\text{Dyson}}(x_1)$, reads

$$\psi^{\text{Dyson}}(x_1) = \int \Psi_N(x_1, x_2, x_3, ..., x_N)\Psi^*_{N-1}(x_2, x_3, x_4, ..., x_N)\, dx_2\, dx_3\, dx_4 ... dx_N \quad (1)$$

where x_i is the space-spin coordinate of electron i. The present P3 calculations employed the diagonal approximation of the self-energy and therefore each corresponding Dyson orbital equals a canonical, HF orbital. Subsequent electron propagator calculations with the Brueckner doubles, coupled-cluster reference state confirmed the validity of the P3 description of the Dyson orbitals for anion VEDEs.

Dyson orbitals generated in the P3 calculations were depicted with the aid of MOLDEN.[35]

Pole strengths, p, are a measure of the qualitative validity of perturbative electron propagator methods such as P3. They are defined by

$$p = \int |\psi^{\text{Dyson}}(x_1)|^2\, dx_1 \quad (2)$$

In the uncorrelated, Koopmans's theorem approximation, pole strengths equal unity for all electron binding energies. Perturbative arguments based on this uncorrelated, zeroth order approximation remain valid when pole strengths are greater than 0.80. Low pole strengths indicate the dominance of shake-up (two-hole, one-particle) operators over simple one-electron annihilators.

Results and Discussion

Structures. Geometry optimizations and frequency calculations on the cations were performed at the HF level with the 6-31G(d,p) basis set. Tetrahedral nitrogens and pyramidal oxygens were assumed for the NH_3 R^+ and OH_2 R^+ cations, respectively. Minima were found for all cations.

These structures were used as initial guesses for HF optimization on the anions with the 6-31++G(d,p) basis set. Minima were found for all anions except OH_2F^-, which dissociated to

(14) Ortiz, J. V. *J. Chem. Phys.* **1989**, *91*, 7024.
(15) Ortiz, J. V. *J. Phys. Chem.* **1990**, *94*, 4762.
(16) Moc, J.; Morokuma, K. *Inorg. Chem.* **1994**, *33*, 551.
(17) Trinquier, G.; Daudey, J.-P.; Caruana G.; Madaule, Y. *J. Am. Chem. Soc.* **1984**, *106*, 4794.
(18) Wang, J.; Boyd, R. J. *Can. J. Phys.* **1994**, *72*, 851.
(19) Boldyrev, A. I.; Simons, J. *J. Phys. Chem.* **1992**, *96*, 8840.
(20) Wright, J. S.; McKay, D. *J. Phys. Chem.* **1996**, *100*, 7392.
(21) Boldyrev, A. I.; Simons, J. *J. Phys. Chem.* **1999**, *103*, 3575.
(22) Boldyrev, A. I.; Simons, J. *J. Chem. Phys.* **1992**, *97*, 6621.
(23) Ditchfield, R.; Hehre, W. J.; Pople, J. A. *J. Chem. Phys.* **1971**, *54*, 724.
(24) Hehre, W. J.; Ditchfield, R.; Pople, J. A. *J. Chem. Phys.* **1972**, *56*, 2257.
(25) Hariharan, P. C.; Pople, J. A. *Theor. Chim. Acta* **1973**, *28*, 213.
(26) Clark, T.; Chandrasekhar, J.; Spitznagel, G. W.; Schleyer, P. v. R. *J. Comput. Chem.* **1983**, *4*, 294.
(27) Bartlett, R. J. *Annu. Rev. Phys. Chem.* **1981**, *32*, 359.
(28) Krishnan, R.; Binkley, J. S.; Seeger, R.; Pople, J. A. *J. Chem. Phys.* **1980**, *72*, 650.
(29) Pople, J. A.; Head-Gordon, M.; Raghavachari, K. *J. Chem. Phys.* **1987**, *87*, 5968.
(30) Ortiz, J. V. *J. Chem. Phys.* **1996**, *104*, 7599.
(31) Ortiz, J. V. *Chem. Phys. Lett.* **1998**, *296*, 494.
(32) Ortiz, J. V. *Chem. Phys. Lett.* **1998**, *297*, 193.
(33) Dunning, T. H. *J. Chem. Phys.* **1989**, *90*, 1007.
(34) GAUSSIAN 98 (Revision A2): Frisch, M. J.; Trucks, G. W.; Schlegel, H. B.; Scuseria, G. E.; Robb, M. A.; Cheeseman, J. R.; Zakrzewski, V. G.; Montgomery, J. A., Jr.; Stratmann, R. E.; Burant, J. C.; Dapprich, S.; Millam, J. M.; Daniels, A. D.; Kudin, K. N.; Strain, M. C.; Farkas, O.; Tomasi, J.; Barone, V.; Cossi, M.; Cammi, R.; Mennucci, B.; Pomelli, C.; Adamo, C.; Clifford, S.; Ochterski, J.; Peterson, G. A.; Ayala, P. Y.; Cui, Q.; Morokuma, K.; Malick, D. K.; Rabuck, A. D.; Raghavachari, K.; Foresman, J. B.; Cioslowski, J.; Ortiz, J. V.; Stefanov, B. B.; Liu, G.; Liashenko, A.; Piskorz, P.; Komaromi, I.; Gomperts, R.; Martin, R. L.; Fox, D. J.; Keith, T.; Al-Laham, M. A.; Peng, C. Y.; Nanayakkara, A.; Gonzalez, C.; Challacombe, M.; Gill, P. M. W.; Johnson, B.; Chen, W.; Wong, M. W.; Andres, J. L.; Head-Gordon, M.; Replogle, E. S.; Pople, J. A. Gaussian, Inc.: Pittsburgh, PA, 1998.
(35) Schaftenaar, G. MOLDEN, CAOS/CAMM Center, The Netherlands, 1998.

the $OH_2 + F^-$ limit. The results of these calculations on $NH_3R^{\pm}$ and $OH_2R^{\pm}$ are given in Tables S1−S11 of the Supporting Information.

The $NH_3R^{\pm}$ ions were transition states when the geometry was optimized with hydrogens of the R substituents eclipsing those of the central, tetrahedral nitrogen, but the optimizations produced true minima when the hydrogens were staggered. Several $OH_2R^{\pm}$ ions had multiple transition states, but only the ions with R = OH produced more than one minimum. One OH_2OH^+ isomer had an H−O−O−H dihedral angle of approximately 120°, while the other had an angle of approximately 60°. For OH_2OH^-, a minimum resembling the former cationic structure was found easily. The other minimum was obtained from an initial guess with a shorter O−O distance.

Averages of cation and anion structures were used as initial guesses for unrestricted HF optimizations on neutrals. Frequency calculations revealed that one optimized structure, for NH_3F, was a transition state corresponding to a collision complex. No minima were found for OH_2F or OH_2OH; minima were obtained for the remaining neutrals.

MP2/6-311++G(d,p) optimizations were initiated at the HF minima. Neutrals and anions dissociated at the MP2 level for all species in which only the neutrals (NH_3F, OH_2OH) had dissociated with HF. The only anomalous result at the MP2 level occurred with the OH_2NH_2 molecule. Here, the corresponding cation and anion optimized to minima, but the neutral molecule dissociated.

Optimizations and frequency calculations were started at the QCISD level with the 6-311++G(d,p) basis set using the MP2 geometries as initial guesses. Only for $OH_2NH_2^-$ was there qualitative disagreement between the MP2 and QCISD results, for in the latter optimization, no minimum was found. Optimized energies and zero-point energies (ZPEs) are shown in Tables 1 and 2, respectively. Adiabatic ionization energies of the neutrals were calculated by finding the differences in energy between the neutrals and their respective cations. These values were corrected with the ZPEs found in the frequency calculations (see Table 3).

Single-point energy calculations were performed on neutral molecules at the geometries of the corresponding anions (see Table 4). Differences between neutral total energies at the optimized anion and neutral geometries define REs of the neutrals (see Table 5).

Electron Binding Energies. When the 6-311++G(2df,2p) basis with extra diffuse functions was used with the P3 method at the anion geometries, VEDEs of all six candidate anions were positive (see Table 6; pole strengths are listed in parentheses beneath each propagator prediction). The largest VEDEs obtain when R = H. For NH_3R^-, the VEDE declines in this order of R: H > OH > NH_2 > CH_3. Since pole strengths of the P3 electron propagator were approximately 0.8 or 0.9, there is little shake-up character in the neutral state in terms of the configuration of the anion. Comparison of P3 and Koopmans's theorem results shows that electron correlation is responsible for a substantial portion of each VEDE. Electron propagator calculations with a Brueckner doubles, coupled-cluster reference state[31,32] and the aug-cc-pVTZ basis[33] with an extra set of s, p, d, and f diffuse functions on the heavy atoms and an extra set of s, p, and d diffuse functions on the hydrogens produce VEDEs of 0.49 eV for NH_4^- and 0.53 eV for OH_3^-. Additional diffuse functions did not yield significant changes in these values. It is likely that employment of the same method for other anions will produce slight increases in VEDEs with respect to those in Table 6.

Table 1. Optimized Energies (au)

	HF	MP2	QCISD
NH_4^+	−56.54553	−56.75569	−56.77247
NH_4	−56.69366	−56.91784	−56.93447
NH_4^-	−56.67211	−56.91717	−56.93719
NH_3F^+	−155.27481	−155.71258	−155.72888
NH_3F	dissociated	dissociated	dissociated
NH_3F^-	−155.40692	dissociated	dissociated
NH_3OH^+	−131.32411	−131.75121	−131.77059
NH_3OH	−131.47172	−131.91223	−131.93110
NH_3OH^-	−131.44588	−131.91035	−131.93242
$NH_3NH_2^+$	−111.53634	−111.93572	−111.96071
NH_3NH_2	−111.67555	−112.08933	−112.11394
$NH_3NH_2^-$	−111.64643	−112.08522	−112.11213
$NH_3CH_3^+$	−95.58887	−95.95096	−95.98214
NH_3CH_3	−95.71949	−96.09703	−96.12801
$NH_3CH_3^-$	−95.69032	−96.09107	−96.12493
OH_3^+	−76.31032	−76.55011	−76.55952
OH_3	−76.48534	−76.74357	−76.75209
OH_3^-	−76.46573	−76.74417	−76.75557
OH_2F^+	−174.96831	−175.43692	−175.44869
OH_2F	dissociated	dissociated	dissociated
OH_2F^-	dissociated	dissociated	dissociated
anti OH_2OH^+	−151.05235	−151.50678	−151.52206
anti OH_2OH	dissociated	dissociated	dissociated
anti OH_2OH^-	−151.18062	dissociated	dissociated
syn OH_2OH^+	−151.04270	−151.49553	−151.51099
syn OH_2OH	dissociated	dissociated	dissociated
syn OH_2OH^-	−151.18703	dissociated	dissociated
$OH_2NH_2^+$	−131.28470	−131.70881	−131.72923
OH_2NH_2	−131.44311	dissociated	dissociated
$OH_2NH_2^-$	−131.40950	−131.88099	dissociated
$OH_2CH_3^+$	−115.35744	−115.74494	−115.77017
OH_2CH_3	−115.50438	−115.91271	−115.93698
$OH_2CH_3^-$	−115.47038	−115.90061	−115.92804

REs were subtracted from P3 VEDEs to produce anion AEDEs (see Table 7). For all six anions that were minima at the QCISD//6-311++G(d,p) level, VEDEs and AEDEs are positive.

Dyson Orbitals. Dyson orbitals corresponding to the P3 results are shown in the figures. The Dyson orbital for the VEDE of NH_4^- consists chiefly of a 2s orbital on N that is surrounded by a diffuse envelope of the opposite phase. Figure 1 displays the ±0.025 contours. Along the N−H bonds, close to the H nuclei, nodes occur between N and H. Electron density associated with this a_1 orbital occurs chiefly outside of the ammonium core. A weak antibonding relationship between N and H is responsible for the minor bond contraction that accompanies electron detachment from the anion. In the united atom limit, this orbital correlates with 3s of Na^-.

For the corresponding Dyson orbital of OH_3^-, a 2s−2p hybrid on O has a similar antibonding relationship with enveloping functions of opposite phase. Figure 2 shows the ±0.035 contours. Along the O−H bond, nodes occur just on the interior side of the H nuclei, as was the case with NH_4^-.

Dyson orbitals for the VEDEs of NH_4^- and OH_3^- calculated with the Brueckner doubles, coupled-cluster reference state are expressed as a linear combination of Brueckner orbitals. The coefficient of one Brueckner orbital is essentially unity and this orbital strongly resembles the Dyson orbital (that is, the canonical HF orbital) of the P3 calculations.

For the NH_3 R^- minima, the most important contributions to the Dyson orbital are made by diffuse s functions on the three hydrogens attached to the four-coordinate nitrogen (see Figures

Table 2. Zero-Point Energies (au)

	HF	MP2	QCISD
NH_4^+	0.05297	0.05014	0.05017
NH_4	0.04929	0.04649	0.04510
NH_4^+	0.04959	0.04419	0.04517
NH_3F^+	0.04601	0.04279	0.04281
NH_3F	dissociated	dissociated	dissociated
NH_3F^-	0.04143	dissociated	dissociated
NH_3OH^+	0.05937	0.05539	0.05548
NH_3OH	0.05571	0.04903	0.04961
NH_3OH^-	0.05618	0.04914	0.05067
$NH_3NH_2^+$	0.07331	0.06904	0.06905
NH_3NH_2	0.07050	0.06393	0.06444
$NH_3NH_2^-$	0.07068	0.06366	0.06490
$NH_3CH_3^+$	0.08463	0.08046	0.08024
NH_3CH_3	0.08191	0.07570	0.07594
$NH_3CH_3^-$	0.08237	0.07604	0.07673
OH_3^+	0.03692	0.03502	0.03525
OH_3	0.03123	0.02673	0.02736
OH_3^-	0.03138	0.02562	0.02706
OH_2F^+	0.02954	0.02703	0.02726
OH_2F	dissociated	dissociated	dissociated
OH_2F^-	dissociated	dissociated	dissociated
anti OH_2OH^+	0.04316	0.04020	0.03988
anti OH_2OH	dissociated	dissociated	dissociated
anti OH_2OH^-	0.03571	dissociated	dissociated
syn OH_2OH^+	0.04228	0.03976	0.03988
syn OH_2OH	dissociated	dissociated	dissociated
syn OH_2OH^-	0.03635	dissociated	dissociated
$OH_2NH_2^+$	0.05689	0.05375	0.05373
OH_2NH_2	0.04869	dissociated	dissociated
$OH_2NH_2^-$	0.05290	0.04171	dissociated
$OH_2CH_3^+$	0.06843	0.06542	0.06529
OH_2CH_3	0.06343	0.05725	0.05757
$OH_2CH_3^-$	0.06515	0.05757	0.05895

Table 3. Adiabatic Ionization Energies (eV)[a]

	MP2	QCISD
NH_4	4.492	4.546
NH_3F	d	d
NH_3OH	4.554	4.528
NH_3NH_2	4.319	4.295
NH_3CH_3	4.104	4.086
OH_3	5.490	5.455
OH_2F	d	d
anti OH_2OH	d	d
syn OH_2OH	d	d
OH_2NH_2	d	d
OH_2CH_3	4.788	4.750

[a] d = dissociated.

3−5). Valence s and p functions on the four-coordinate nitrogens produce lobes with opposite phase that point toward the three hydrogens. As with NH_4^-, nodes occur close to the three hydrogens that are bound to the nitrogen. Smaller valence s and p contributions are present on the non-hydrogen atoms of the R groups. Minor lobes establish a bonding relationship between the four-coordinate nitrogen and the other non-hydrogen nuclei.

In $OH_2CH_3^-$, the Dyson orbital has large contributions from diffuse s functions on the two hydrogens attached to the three-coordinate oxygen (see Figure 6). These functions have an out-of-phase relationship with a hybrid centered on the three-coordinate oxygen. The minor lobe of a carbon-centered hybrid orbital points indirectly toward the oxygen. This bonding pattern recapitulates the relationships seen in the $NH_3CH_3^-$ Dyson orbital.

Table 4. Neutral Energies at Anion Geometries (au)

	HF	MP2	QCISD
NH_4	−56.69363	−56.91777	−56.93447
NH_3F	−155.43296	ad	ad
NH_3OH	−131.47162	−131.91205	−131.93100
NH_3NH_2	−111.67543	−112.08911	−112.11381
NH_3CH_3	−95.71943	−96.09696	−96.12796
OH_3	−76.48527	−76.74322	−76.75197
OH_2F	ad	ad	ad
OH_2OH #1	−151.21710	ad	ad
OH_2OH #2	−151.21541	ad	ad
OH_2NH_2	−131.44178	−131.88793	ad
OH_2CH_3	−115.50420	−115.91235	−115.93663

[a] ad = anion dissociated.

Table 5. Neutral Relaxation Energies (eV)[a]

	HF	MP2	QCISD
NH_4	0.001	0.002	0.000
NH_3F	nd	ad	ad
NH_3OH	0.003	0.005	0.000
NH_3NH_2	0.003	0.006	0.004
NH_3CH_3	0.002	0.002	0.000
OH_3	0.002	0.010	0.003
OH_2F	ad	ad	ad
anti OH_2OH	nd	ad	ad
syn OH_2OH	nd	ad	ad
OH_2NH_2	0.036	nd	ad
OH_2CH_3	0.005	0.010	0.010

[a] ad = anion dissociated; nd = neutral dissociated.

Table 6. Vertical Electron Detachment Energies (eV)

anion	Koopmans	P3	BD-EPT
$NH_3CH_3^-$	0.12	0.34	
		(0.82)	
$NH_3NH_2^-$	0.14	0.40	
		(0.84)	
NH_3OH^-	0.18	0.41	
		(0.84)	
NH_4^-	0.22	0.44	0.49
		(0.87)	(0.86)
$OH_2CH_3^-$	0.12	0.24	
		(0.79)	
OH_3^-	0.31	0.46	0.54
		(0.85)	(0.86)
NH_3F^-		dissociated	
$OH_2NH_2^-$		dissociated	
anti OH_2OH^-		dissociated	
syn $OH_2OH_2^-$		dissociated	
OH_2F^-		dissociated	

Table 7. Adiabatic Electron Detachment Energies (eV)

anion	AEDE	anion	AEDE
$NH_3CH_3^-$	0.34	NH_4^-	0.44
$NH_3NH_2^-$	0.36	$OH_2CH_3^-$	0.14
NH_3OH^-	0.41	OH_3^-	0.43

When R = NH_2, diffuse orbital contributions are largest on the hydrogen covalently bound to the four-coordinate N which is closest to the two hydrogens of the amino group. For NH_3OH^-, smaller diffuse contributions are made by the hydrogen which is anti with respect to the hydroxide hydrogen.

In all cases, Dyson orbitals are dominated by the most diffuse basis functions and nodes occur between the central N or O nucleus and the neighboring hydrogens. Plots of these orbitals corroborate the double-Rydberg description of the two least bound electrons. One may expect sharp peaks for electron detachment from these double-Rydberg anions.

Bond lengths between the central nitrogen or oxygen atoms

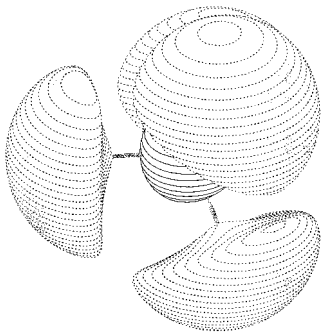

Figure 1. Dyson orbital for VEDE of NH_4^-; contour = ±0.025.

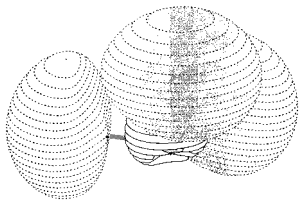

Figure 2. Dyson orbital for VEDE of OH_3^-; contour = ±0.035.

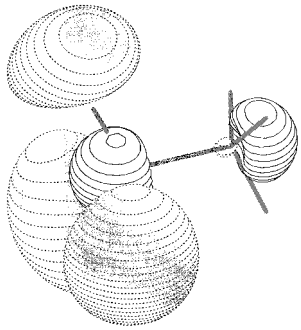

Figure 3. Dyson orbital for VEDE of $NH_3CH_3^-$; contour = ±0.025.

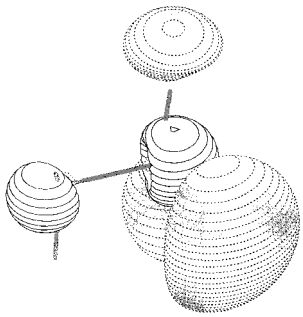

Figure 4. Dyson orbital for VEDE of $NH_3NH_2^-$; contour = ±0.0275.

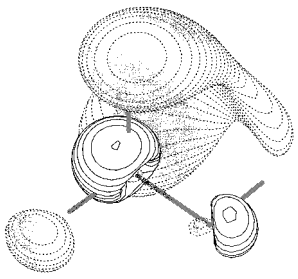

Figure 5. Dyson orbital for VEDE of NH_3OH^-; contour = ±0.030.

and their neighboring hydrogens are larger for anions than for cations. Intermediate values obtain for the neutrals. This trend is compatible with the N−H and O−H antibonding phase relationship seen in the Dyson orbitals.

The bonding relationship between the minor lobes of the s−p valence hybrids on the non-hydrogen atoms in $NH_3CH_3^-$ and $OH_2CH_3^-$ explains why N−C and O−C bond lengths are longer in the cations than in the anions. Neutral N−C and O−C bond lengths lie between the anion and cation values. These bond length effects are small. Similarities between neutral and anionic geometries remain strong.

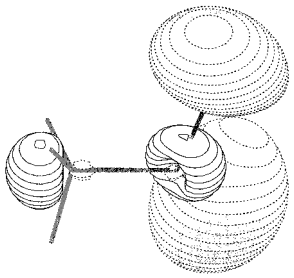

Figure 6. Dyson orbital for VEDE of $OH_2CH_3^-$; contour = ±0.0325.

Electron Correlation. Analysis of electron propagator results on NH_4^- and OH_3^- with the Brueckner doubles reference state provides additional insights into electron correlation effects on the VEDEs. For each calculated VEDE, there is a corresponding linear combination of operators that acts on the anion reference state to produce an uncharged species. The large pole strengths of Table 6 indicate that the dominant operators (with coefficients near 0.9) pertain to annihilation of a single electron in an occupied orbital. Next in importance (with coefficients between 0.1 and 0.2) are two-particle, one-hole ionization operators that annihilate two electrons in the highest occupied molecular orbital and create an electron in a virtual orbital that corresponds to the totally symmetric irreducible representation of the anion's point group. These virtual orbitals consist mostly of s basis functions on the N, O, and H nuclei and they differ from the highest occupied orbital in their radial nodal structure. These two-particle, one-hole ionization operators therefore remove an electron from the highest occupied molecular orbital and promote an electron from the same occupied orbital to a virtual orbital with the same symmetry label.

Such results indicate the importance of orbital relaxation in the neutral final state. After electron detachment from the anion, the remaining electron assigned to the highest occupied orbital contracts. In the uncharged, final state, there is less radial correlation between diffuse electrons.

Related Experiments. Experimentalists already have the means to make many of these anions and the spectroscopic techniques to test predictions. Photoelectron spectra of OH_3^- have provided delicate probes of the two anion−molecule minima, $OH^-(H_2)$ and $H^-(H_2O)$, and of the dynamics of the $OH + H_2 \rightarrow H_2O + H$ reaction.[36,37] Spectra were not reported for electron binding energies near the predicted values (approximately 0.4−0.5 eV[10,13,15]) for the double-Rydberg anion. (Previous predictions on the VEDEs of related anion−molecule complexes were in excellent agreement with experiment[14] and the corresponding structures have been confirmed by subsequent calculations.[38]) There is evidence for more than one form of OH_3^- from charge-inversion, mass spectra.[39] Several other anions are accessible to experiment as well. $O_2H_3^-$ was one of the first anionic clusters to be characterized spectroscopically.[40]

(36) Miller, T. M.; Leopold, D. G.; Murray, K. K.; Lineberger, W. C. *Bull. Am. Phys. Soc.* **1985**, *30*, 880.
(37) De Beer, E.; Kim, E. H.; Neumark, D. M.; Gunion, R. F.; Lineberger, W. C. *J. Phys. Chem.* **1995**, *99*, 13627.
(38) Wang, D.; Zhang J. Z. H.; Yu, C. *Chem. Phys. Lett.* **1997**, *273*, 171.
(39) Griffiths, W. J.; Harris, F. M. *Org. Mass Spectrom.* **1987**, *22*, 812.
(40) Golub, S.; Steiner, B. *J. Chem. Phys.* **1968**, *49*, 5191.

Insights into the transition state of the $OH + H_2O \rightarrow H_2O + OH$ reaction have been obtained through photoelectron spectra of $O_2H_3^-$.[41] $N_2H_5^-$ and $N_2H_7^-$ have been made as well.[3,42] All interpretations to date on these species have assumed anion−molecule structures such as $H^-(OH_2)$, $OH^-(OH_2)$, $NH_2^-(NH_3)$, and $H^-(NH_3)_2$. For these structures, electron detachment energies will exceed those of the corresponding, free anions and therefore will be distinctly larger than their double-Rydberg counterparts.

Conclusions

Two classes of double-Rydberg anions have been investigated. NH_3R^- anions with a tetrahedral nitrogen center and OH_2R^- anions with a tricoordinate, pyramidal oxygen center have been examined for R = H, F, OH, NH_2, and CH_3. Stable minima in the anion potential energy surfaces have been found for NH_4^-, NH_3OH^-, $NH_3NH_2^-$, $NH_3CH_3^-$, OH_3^-, and $OH_2CH_3^-$. All of these minima have positive vertical electron detachment energies. Optimizations on the corresponding neutrals and cations produce similar minima. For all six anions, the adiabatic electron detachment energies are positive. The least bound electrons of the anions are located chiefly outside the nuclear framework, beyond the N−H bonds of the central nitrogens in NH_3R^- and beyond the O−H bonds of the central oxygens in $OH_2CH_3^-$. Attachment of one or two electrons to the corresponding cations leads to slightly longer N−H and O−H bond lengths pertaining to the central atoms. Such electron attachments also decrease bond lengths between central atoms and the non-hydrogen atoms of the R groups.

Acknowledgment. This work was supported by the National Science Foundation under grant CHE-9873897. Hugh Hopper of Millikan College, Johnson City, TN, and Michael Lococo of Bard College, Annandale, NY, also were supported by the National Science Foundation's Research Experiences for Undergraduates program at Kansas State University in the summers of 1998 and 1999, respectively.

Supporting Information Available: Tables of structures and frequencies (PDF). This material is available free of charge via the Internet at http://pubs.acs.org.

JA002292+

(41) Arnold, D. W.; Xu, C.; Neumark, D. M. *J. Chem. Phys.* **1995**, *102*, 6088.

(42) Snodgrass, J. T.; Coe, J. V.; Freidhoff, C. B.; McHugh, K. M.; Arnold, S. T.; Bowen, K. H. *J. Phys. Chem.* **1995**, *99*, 9675.